

Chaotic scattering of electrons with He^+

Yan Gu* and Jian-Min Yuan

Department of Physics and Atmospheric Science, Drexel University, Philadelphia, Pennsylvania 19104

(Received 1 December 1992)

We investigate the classical scattering patterns of an electron off a He^+ ion. The scattering functions exhibit interesting self-similar structure, which can be interpreted in terms of the indefinite number of electronic returns to the vicinity of the nucleus, encounters among the particles, and Kepler-like electronic excursions during the collisional process. Based on this mechanism a binary coding is introduced to organize the dynamics of this three-body system and yields escape rates that vary with the sectional cut in the parameter space. The physical interpretation and the symbolic dynamics introduced here are generally useful for all three-body collisional systems.

PACS number(s): 34.80.Kw, 05.45.+b

The revival of interest in classical and semiclassical studies of three-body Coulomb systems has been stimulated by recent measurements of highly doubly excited atoms and ions [1] as well as the discovery of new stable periodic orbits in atomic helium [2]. These semiclassical studies [3–5] are successful in predicting quantum spectra in terms of periodic orbits, a long-failed goal of the old quantum theory, and providing new insights into a high-energy regime of the spectra. In this regime accurate quantum calculations are hard to come by.

With a few exceptions, most of the classical periodic orbits of a three-body Coulomb system are unstable against autoionization. From another point of view this means that we can explore the full system dynamics by studying the scattering process. Furthermore, recent progress in irregular scattering [6–13] demonstrates that scattering functions often provide us with rich information about the underlying phase-space structure. The objective of this Rapid Communication is to explore such scattering properties of the electron- He^+ ion system in order to gain a deeper intuitive understanding of the dynamics associated with the high-lying metastable states of helium.

Assuming the nucleus is infinitely heavy and fixed at the origin, we focus our attention on the coplanar motion of two electrons. Although approximate, the planar configuration retains most of the essential features of the scattering properties of the system, for which the Hamiltonian in atomic units can be written as

$$H = \frac{1}{2}(P_1^2 + P_2^2) - \frac{Z}{r_1} - \frac{Z}{r_2} + \frac{1}{r_{12}}, \quad (1)$$

where $Z=2$ for atomic helium. Since the potential is a homogeneous function of r_i ($i=1,2$) of degree -1 , the classical dynamics is invariant under an energy scaling transform; it is sufficient to perform calculations at the fixed total energy, $E=-1$ (with reference to the energy of three free stationary particles). Due to this normalization of energy, rotational invariance, and the fixed initial condition that $r_2 = \infty$ when $t = -\infty$, the total number of the initial conditions that must be specified is actually 5.

The high dimensionality of the planar three-body Coulomb system combined with its long-range interaction and singular nature of the potential make the numerical calculations difficult to perform by brute force methods. Ingenious methods must be introduced to obtain solutions accurately. We describe our method below: We divide the plane of motion into three zones by drawing two imaginary concentric circles with radius R_c and r_c , respectively, about the nucleus. Numerical calculations of trajectories are carried out only when both electrons are inside the annular region, i.e., $R_c > r_1, r_2 > r_c$. Since we have normalized the total energy to $E=-1$, for sufficiently large R_c one of the electron's distance from the nucleus will always be far smaller than R_c . On the other hand, for sufficiently small r_c , it is quite unlikely that both r_i 's are of the same order as r_c . Thus it is legitimate and time saving to calculate the trajectories analytically by invoking two-body (or mean-field) approximations. That is, whenever two electrons are in different zones, we propagate the trajectories by assuming that the outer electron is moving in a static Coulomb field with a point charge of $Z-1$, and the inner electron moving in a field of a point charge of Z . For our purpose, we have found that a choice of $R_c=100$ and $r_c=10^5$ in our numerical code (based on a variable-step Runge-Kutta method) can conserve energy to within 10^{-9} for most of the trajectories that we report on below.

We consider the collisional process represented schematically in Fig. 1. The two initial parameters that need to be specified for e_1 are taken to be the initial energy of e_1 , E_1 , and its angle ϕ when e_2 arrives at R_c . Calculated scattering functions, such as the scattering angle θ , collisional time, or energy of the outgoing electron E_{out} , all exhibit interesting self-similar structure. We present in Fig. 2 results for the parameters $E_1=-1.2$ (i.e., $r_1=0.833$) and $\phi=0$. Only results of the collisional time τ_c , defined by the time during which both electrons stay inside the R_c circle, are shown in Fig. 2(a) for 500 equally spaced b values between -5 and 5 . In parts of this close-encountered interval the collisional function looks highly fluctuated. If the function in these fluctuating

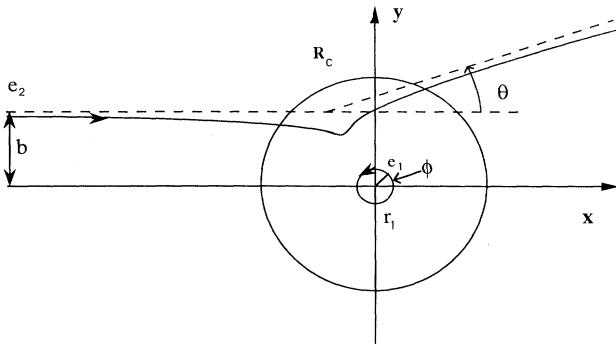


FIG. 1. Schematic drawing of the $e + \text{He}^+$ scattering process, which defines the asymptotic parameters. Electron 1 is initially on a circular Kepler orbit of radius r_1 with a phase ϕ when e_2 arrives at R_c from infinity with an impact parameter b . The scattering angle of the outgoing electron is θ . R_c is defined in the text.

parts is plotted with a finer scale, we again find subdomains of smooth regular behavior, interlaced with highly fluctuating bands. To illustrate this, we enlarge one of the fluctuating regions of Fig. 2(a) for two generations, as shown in Figs. 2(b) and 2(c). In Fig. 2(b), we blow up the chaotic band located from $b = 1.2$ to 2.8 of Fig. 2(a) (1500 points plotted). A very rich structure is

revealed in which a big cusp-shaped interval of regular behavior is located around $b = 1.88$, surrounded by seemingly infinitely many smaller but similar cusp-shaped intervals of regularity, separated by chaotic bands. Moving away from the biggest cusp region the widths and spacings of the cusp intervals converge gradually to zero as they approach the borderline of this entire irregular region (from about 1.2 to 2.8). The borderline of the chaotic band seems to be characterized by infinitesimal escape velocities of the outgoing electrons ($E_{\text{out}} \sim 0$). The cusp points of Fig. 2(b) correspond, on the other hand, to the high values of E_{out} and apparent discontinuities of the scattering angles. A further blowup of the chaotic band $b = 1.70$ to 1.83 is shown in Fig. 2(c) (1200 points). Even richer structure is revealed in this generation. First, self-similarity is clearly shown; that is, all features of the chaotic band discussed above seem to repeat themselves at this level. For instance, Fig. 2(c) shows that the $b = 1.71-1.83$ region is remarkably similar to that of $b = 1.3-2.6$ of Fig. 2(b). Particularly, the hierarchy of cusp-shaped regions discussed above about Fig. 2(b) appears at this level too. Further blowups reveal that these features of the chaotic bands repeat themselves at all levels. Another interesting phenomenon that becomes apparent in Fig. 2(c) is that the tips of the cusp seem to reveal further irregular structure.

To understand these features, particularly, the self-similarity of cusp-shaped intervals, we should examine individual trajectories. Plotted in Fig. 3 are the trajectories of e_1 and e_2 in the xy plane corresponding to two different b values, 1.849 and 1.896, which are located at the opposite sides of the biggest regular interval of Fig. 2(b). The obvious difference between these two trajectories is that in the case of $b = 1.849$ both the projectile

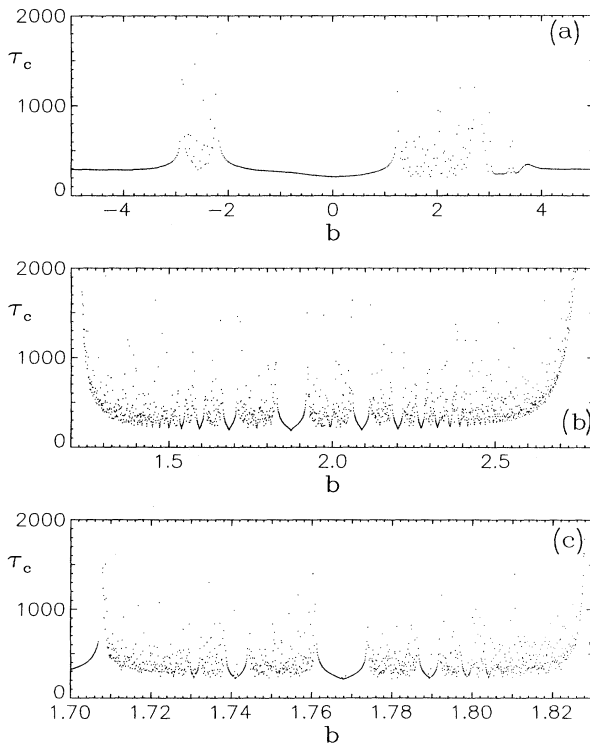


FIG. 2. Collisional time τ_c as a function of b for the initial conditions $E_1 = -1.2$ and $\phi = 0^\circ$ (total energy $E = -1$). (a) For $-5 < b < 5$. (b) Blowup of (a) for the range $1.2 < b < 2.8$. (c) Further blowup for the range $1.70 < b < 1.83$.

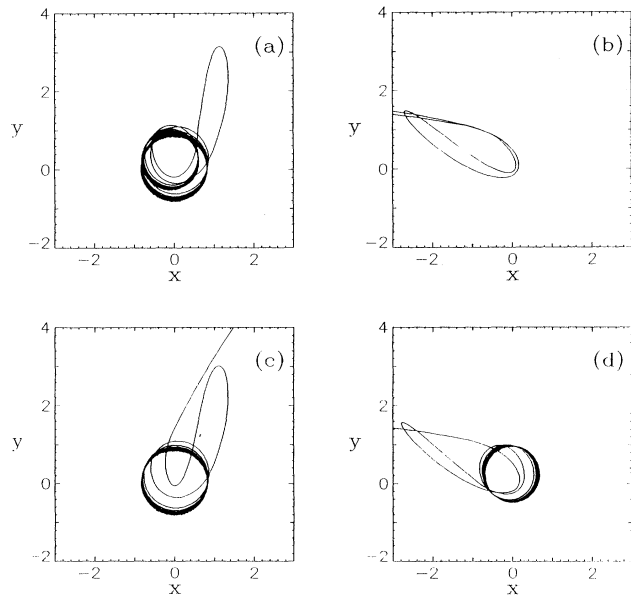


FIG. 3. Scattering trajectories of electrons. (a) Trajectory of e_1 at $b = 1.849$. (b) Trajectory of e_2 at $b = 1.849$. (c) Trajectory of e_1 at $b = 1.896$. (d) Trajectory of e_2 at $b = 1.896$.

and the escape electrons are e_2 , namely, no net exchange occurs as a consequence of collision. In the case of $b = 1.896$, exchange does occur, so that the outgoing electron is e_1 . This fact that trajectories from the opposite sides of the same regular interval differ in the outgoing electrons seems to be a general feature of all the regular intervals at all levels.

To see why infinitely many cusp intervals show up in the second generation of plotting as shown in Fig. 2(b), we plot in Figs. 4(a) and 4(b) the trajectories for $b = 1.67$. This b value can be found at the left branch of the left one of the two second biggest cusp-shaped intervals of the chaotic band of Fig. 2(b). We observe that the trajectory of e_1 shown in Fig. 4(a) resembles that of Fig. 3(a), except that the excursion goes farther out from the nucleus, while e_2 shown in Fig. 4(b) comes to the vicinity of the nucleus for a third time, as compared to only twice in Fig. 3(b). This example suggests that when the b value is varied from the central cusp to the smaller and smaller regular cusps within a chaotic band, the more energetic electron is making a longer and longer excursion away from the nucleus. Meanwhile the less energetic electron makes more and more trips around the nucleus before the two electrons collide again. This is the mechanism responsible for the appearance of the infinite sequences of the cusp-shaped intervals within a chaotic band. The convergence of the interval widths and spacings to zero when b approaches the boundary of the chaotic band is related to the fact that the ratio of the periods around the nucleus of the less over the more energetic electrons approaches zero, for the latter period goes to infinity at the band boundary.

Finally, to understand what happens when we move down to the next generation within a chaotic band, we plot in Figs. 4(c) and 4(d) the trajectories for $b = 1.74$, be-

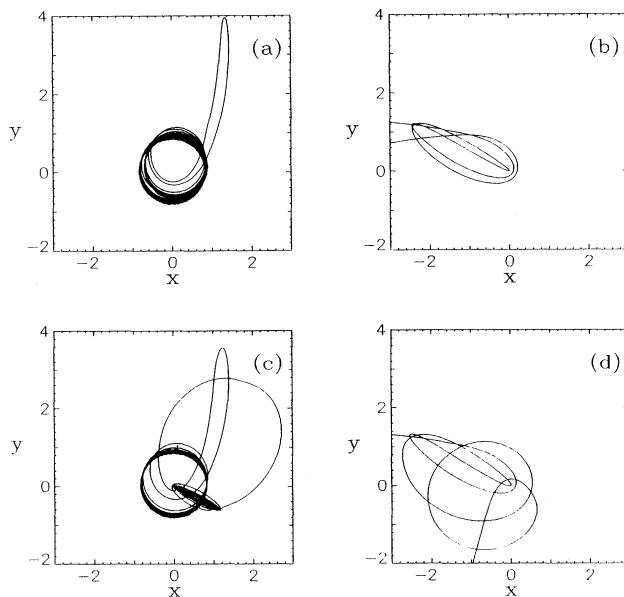


FIG. 4. Scattering trajectories of electrons. (a) Trajectory of e_1 at $b = 1.670$. (b) Trajectory of e_2 at $b = 1.670$. (c) Trajectory of e_1 at $b = 1.740$. (d) Trajectory of e_2 at $b = 1.740$.

longing to a cusp interval of the third generations [Fig. 2(c)]. An obvious difference between the trajectories shown in Figs. 4(a) and 4(c) is that in Fig. 4(c) e_1 (the more energetic electron of the two here) executes one more long excursion away from the nucleus than that of Fig. 4(a). Therefore, the number of long excursions made by the more energetic electron from the nucleus determines the generation to which a certain trajectory belongs. To summarize, we observe that two electrons can experience an indefinite number of returns and encounters as well as Kepler-like excursions during the collisional process, which explains why the scattering functions exhibit hierarchy of self-similar structure. Since similar hierarchical structure has been observed in various three-body collisional systems including atom-diatom [6] and binary-single star collisions [12], the physical interpretation presented here could be the general underlying mechanism for all three-body collisional systems.

The self-similar structure exhibited by various scattering functions is often the common feature of chaotic scattering [6–13]. This structure can be interpreted in the most straightforward way by using symbolic dynamics. But for systems beyond simple potential scattering it is a nontrivial matter to construct such a system of symbolic dynamics. We discuss below the symbolic system that we have developed for the present three-body problem. From the foregoing discussions, we know that the ever finer structure of the scattering function is due to the ever-growing number of excursions of electrons to a distance far away from the nucleus, taking place during a collisional process. To quantify this idea of excursion, we shall introduce the terminology, “return of the energetically favored particle,” which describes the event in which the electron with greater energy changes its radial momentum from a positive to a negative value. A symbolic word is formed by taking the labels (1 or 2) of the energetically favored electron, which happens to change its sign of the radial momentum, and arranging them in the order of time. Attaching at the beginning of the word the label for the incoming electron and at the end that of the outgoing electron, we form a symbolic word for an individual trajectory. For examples, the trajectories depicted in Figs. 3(a) and 3(b), 3(c) and 3(d), and 4(a) and 4(b) are labeled, respectively, by 212, 211, and 212. They all belong to the regular intervals in the second generation [Fig. 2(b)]. The other example, Figs. 4(c) and 4(d), has a symbol of 2112 to describe the fact that the e_1 returns twice to the neighborhood of the nucleus when it becomes energetically favored, but eventually it becomes permanently trapped in the bound region. Thus it belongs to a regular interval in the third generation [Fig. 2(c)]. The advantage of using the local returns to define the symbolic sequence is that it can be easily determined while the trajectory is being calculated.

Using this scheme we have determined the symbolic sequences for all the trajectories studied, which amounts to several thousands of them. We have found that this symbolic dynamics cleanly organizes the hierarchical structure of the three-body collisional system, both the horizontal structure across the bi-infinite sequence within a single generation and the vertical structure going down

the generations. For example, if we divide the regular intervals of Fig. 2(b) into two infinite sequences, one sequence each on the left- and right-hand sides (lhs and rhs) of the central cusp, focusing on the left infinite sequence, which converges to the left end of the chaotic band around $b = 1.1$, we find that all the regular intervals (including the central cusp) of this sequence are coded by 212 on the lhs of the cusps and 211 on the rhs. All codes begin with 21, the code for the left band boundary. On the other hand, all the regular intervals of the right sequence are coded by 222 on the lhs of the cusps and 221 on the rhs. All codes here begin with 22, the code for the rhs boundary. Similar rules apply when we go down to the next generation; for example, to the level of Fig. 2(c). The chaotic band in the figure borders on a 211 regular interval on the left and a 212 interval on the right. We find that this time all the regular intervals of the left infinite sequence are labeled by 2112 on the lhs of each cusp and 2111 on the rhs. In the right sequence, all the regular intervals (including the central one) have the code 2122 on the lhs of the cusp and 2121 on the rhs. As with the physical mechanism the symbolic dynamics introduced here should be generally useful for all three-body collisional systems, for they seem to show similar hierarchical structure.

Despite the success of the symbolic dynamics adopted here, several exceptions have also been unearthed. For instance, we have discovered that a regular interval may have two different symbolic sequences. This mislabeling of the interval occurs only in the following two cases. (1) The energetically favored electron has small radial fluctuations. (2) The two electrons have approximately the same amount of energy when one of them returns. Since these exceptions rarely occur, they will not affect the statistical results in the study of the scaling behavior of the self-similarity, discussed below.

Figure 2 seems to indicate the existence of a set of b values on which the scattering functions become singular. This set resembles the Cantor set, generated by removing a certain fraction of a solid line repeatedly at all levels. The equivalent process in our problem is to remove first the regular cusp intervals from the b axis at the level of

Fig. 2(a), then regular intervals at the level of Fig. 2(b), and *ad infinitum*. A difference in the present case from the Cantor set is that at each level an infinite number of regular intervals are removed and the widths and spacings of the regular intervals converge to zero towards both ends of the chaotic band. To characterize quantitatively the dynamics and the remaining fractal set, we have run an ensemble of trajectories and calculated the number of trajectories surviving (N) after removing the trajectories lying inside the n th-level regular intervals. These trajectories are labeled by words with the code length equal to $n + 1$ in our notation. A linear relationship is obtained when we plot $\log(N)$ versus n for three sets of data, corresponding to the following initial conditions: (1) $E_1 = -1.2$, $\phi = 0^\circ$; (2) $E_1 = -1.2$, $\phi = 60^\circ$; and (3) $E_1 = -2.0$, $\phi = 0^\circ$. To generate each data set, about 6000 to 7000 equally spaced b values are scanned. The survival probability is therefore an exponential function of n as given by $P(n) = N(n)/N(1) = \exp[-\alpha(n-1)]$. The α values obtained by the least-squares method are, respectively, 0.486, 0.447, and 0.405, which has the physical meaning of the escape rate that measures the average instability of the chaotic repellers of the system. The fractal dimensions of the corresponding surviving trajectories [7] are calculated to be 0.588, 0.608, and 0.631, respectively. The fact that the α value varies (by 20% here) according to where one cuts through the three-dimensional parameter space (E_1, ϕ, b) is particularly significant, because it is believed that the Hamiltonian invariant set is isotropic multifractals [13]. However, our results suggest that the invariant set of the present system may consist of several disjoint parts, so that the phase space is not ergodic.

We are grateful to Tamás Tél, Stephen L. W. McMillan, Patricia T. Boyd, and Michel Vallieres for stimulating discussions. Acknowledgment is made to the Donors of the Petroleum Research Fund, administered by the American Chemical Society, for support of this research. One of us (Y.G.) also acknowledges the National Basic Research Project "Nonlinear Science" for its partial support of this work.

- *Permanent address: Center for Fundamental Physics, University of Science and Technology of China, Hefei, 230026, China.
- [1] U. Eichmann, V. Lange, and W. Sandner, Phys. Rev. Lett. **64**, 274 (1990); **68**, 21 (1992); L. G. Harris *et al.*, Phys. Rev. **42**, 6443 (1990); M. Domke *et al.*, Phys. Rev. Lett. **66**, 1306 (1991).
 - [2] K. Richter and W. Wintgen, J. Phys. B **23**, L197 (1990); Phys. Rev. Lett. **65**, 1965 (1990).
 - [3] G. Ezra, K. Richter, G. Tanner, and D. Wintgen, J. Phys. B **24**, L413 (1991).
 - [4] R. Blümel and W. P. Reinhardt, in *Directions in Chaos*, edited by D. H. Feng and J. M. Yuan (World Scientific, Singapore, 1992), Vol. 4, p. 245.
 - [5] J. Müller, J. Burgdörfer, and D. W. Noid, Phys. Rev. A **45**, 1471 (1992).

- [6] D. W. Noid, S. Gray, and S. A. Rice, J. Chem. Phys. **85**, 2649 (1986).
- [7] B. Eckhardt, Physica D **33**, 89 (1988); J. Phys. A **20**, 5971 (1987).
- [8] R. Blümel and U. Smilansky, Phys. Rev. Lett. **60**, 477 (1988).
- [9] P. Gaspard and S. A. Rice, J. Chem. Phys. **90**, 2225 (1989).
- [10] S. Bleher, C. Grebogi, and E. Ott, Physica D **46**, 87 (1990).
- [11] Z. M. Lu, M. Vallieres, J. M. Yuan, and J. F. Heagy, Phys. Rev. A **45**, 5512 (1992).
- [12] P. Boyd and S. W. McMillan, Phys. Rev. A **46**, 6277 (1992).
- [13] T. Tél, in *Directions in Chaos: Experimental Study and Characterization of Chaos*, edited by Hao B. L. (World Scientific, Singapore, 1990), Vol. 3, p. 149.